PROC. OF JSCE,
NO. 220, DEC. 1973

FINITE DIFFERENCE ANALYSIS OF CIRCULAR RING SECTOR PLATES SUPPORTED BY EDGE-BEAMS

*By Hisanori OTSUKA**

1. INTRODUCTION

The development of the modern highway system has required an increasing number of curved bridges. The superstructures of these curved highway bridges may be treated in many cases as the circular ring sector plates supported by edge-beams.

It will be useful to investigate the influences of supporting conditions at the corner points of these plates, flexural and torsional rigidities of the edge-beams and opening angles of the plates on deflections and internal forces of the bridges.

This paper presents a finite difference analysis of circular ring sector plates with edges elastically supported by beams. Since complicated boundary conditions may prevent the expression of exact solutions, finite difference techniques are adopted in this study. The plate treated herein is analysed using small deformation, thin plate theory. Numerical computations for many typical cases are also carried out and the mechanical characteristics of these plates are studied.

2. METHOD OF ANALYSIS

(1) Fundamental Equations of Sector Plates

The governing equation of plate theory, in polar coordinates, is

$$\Delta^2 w = p/D \quad \cdots\cdots(1)$$

where w is the deflection of the plate, p is the intensity of the applied load, D is the flexural rigidity of the plate per unit width, and Δ is the Laplacian operator:

$$\Delta = \frac{\partial^2}{\partial r^2} + \frac{1}{r}\frac{\partial}{\partial r} + \frac{1}{r^2}\frac{\partial^2}{\partial \theta^2}$$

The bending moments and reaction forces of the plate are given by

$$M_r = -D\left[\frac{\partial^2 w}{\partial r^2} + \nu\left(\frac{1}{r}\frac{\partial w}{\partial r} + \frac{1}{r^2}\frac{\partial^2 w}{\partial \theta^2}\right)\right] \quad \cdots\cdots(2)$$

$$M_\theta = -D\left[\frac{1}{r}\frac{\partial w}{\partial r} + \frac{1}{r^2}\frac{\partial^2 w}{\partial \theta^2} + \nu\frac{\partial^2 w}{\partial r^2}\right] \quad \cdots(3)$$

$$V_r = -D\left[\frac{\partial^3 w}{\partial r^3} - \frac{1}{r^2}\frac{\partial w}{\partial r} + \frac{1}{r}\frac{\partial^2 w}{\partial r^2} - \frac{3-\nu}{r^3}\frac{\partial^2 w}{\partial \theta^2} + \frac{2-\nu}{r^2}\frac{\partial^3 w}{\partial r \partial \theta^2}\right] \quad \cdots\cdots(4)$$

$$V_\theta = -D\left[\frac{1}{r^3}\frac{\partial^3 w}{\partial \theta^3} + \frac{2}{r^3}(1-\nu)\frac{\partial w}{\partial \theta} + \frac{2-\nu}{r}\frac{\partial^3 w}{\partial r^2 \partial \theta} + \frac{2\nu-1}{r^2}\frac{\partial^2 w}{\partial r \partial \theta}\right] \quad \cdots(5)$$

in which M_r, M_θ, V_r and V_θ are the radial bending moment, tangential bending moment, radial reaction and tangential reaction per unit length of the plate, respectively.

The network chosen for this study contains $(m+1)$ by $(n+1)$ mesh points as shown in Fig. 1.

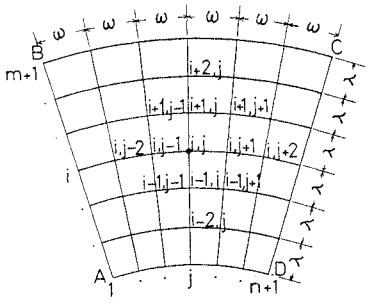

Fig. 1 Finite Difference Network for Sector Plate

Eq. (1) can be transformed into the following finite difference equation for this network:

* Doctoral Course Student, Department of Civil Engineering, Kyushu University.

$$\left\{\begin{array}{ccccc} & & a_1 & & \\ & a_2 & a_3 & a_2 & \\ a_4 & a_5 & a_6 & a_5 & a_4 \\ & a_7 & a_8 & a_7 & \\ & & a_9 & & \end{array}\right\} W=\frac{p\lambda^4}{D} \quad \cdots(6)$$

where

$a_1=1+\lambda/r_i$
$a_2=2\kappa^2(1-\lambda/2r_i)/r_i^2$
$a_3=-4(1+\lambda/2r_i)-(1-\lambda/2r_i)(\lambda^2+4\kappa^2)/r_i^2$
$a_4=\kappa^4/r_i^4$
$a_5=-4\kappa^2\{1-(\lambda^2-\kappa^2)/r_i^2\}/r_i^2$
$a_6=2\{3+(\lambda^2+4\kappa^2)/r_i^2-\kappa^2(4\lambda^2-3\kappa^2)/r_i^4\}$
$a_7=2\kappa^2(1+\lambda/2r_i)/r_i^2$
$a_8=-4(1-\lambda/2r_i)-(1+\lambda/2r_i)(\lambda^2+4\kappa^2)/r_i^2$
$a_9=1-\lambda/r_i$
$\lambda=l/m$, $\omega=\theta_0/n$, $\kappa=\lambda/\omega$.

Expressions of bending moment and reaction force, i.e. Eqs. (2) to (5), may also be transformed into finite difference equations shown by Eqs. (7) to (10), respectively:

$$M_r=\left\{\begin{array}{ccccc} & & b_1 & & \\ & b_2 & b_3 & b_2 & \\ & & b_4 & & \end{array}\right\} W \quad \cdots\cdots(7)$$

where

$b_1=-D(1+\nu\lambda/2r_i)/\lambda^2$
$b_2=-D\nu\kappa^2/\lambda^2r_i^2$
$b_3=2D(1+\nu\kappa^2/r_i^2)/\lambda^2$
$b_4=-D(1-\nu\lambda/2r_i)/\lambda^2$

$$M_\theta=\left\{\begin{array}{ccccc} & & \bar{b}_1 & & \\ & \bar{b}_2 & \bar{b}_3 & \bar{b}_2 & \\ & & \bar{b}_4 & & \end{array}\right\} W \quad \cdots\cdots(8)$$

where

$\bar{b}_1=-D(\nu+\lambda/2r_i)/\lambda^2$
$\bar{b}_2=-D\kappa^2/\lambda^2r_i^2$
$\bar{b}_3=2D(\nu+\kappa^2/r_i^2)/\lambda^2$
$\bar{b}_4=-D(\nu-\lambda/2r_i)/\lambda^2$

$$V_r=\left\{\begin{array}{ccccc} & & c_1 & & \\ & c_2 & c_3 & c_2 & \\ c_4 & c_5 & c_4 & & \\ & c_2 & c_6 & c_2 & \\ & & c_1 & & \end{array}\right\} W \quad \cdots\cdots(9)$$

where

$c_1=-D/2\lambda^3$
$c_2=-D\kappa^2(2-\nu)/2\lambda^3r_i^2$
$c_3=D\{1-\lambda/r_i+\lambda^2/2r_i^2+(2-\nu)\kappa^2/r_i^2\}/\lambda^3$
$c_4=(3-\nu)D\kappa^2/\lambda^2r_i^3$
$c_5=2D\{1-(3-\nu)\kappa^2/r_i^2\}/\lambda^2r_i$
$c_6=-D\{1+\lambda/r_i+\lambda^2/2r_i^2+(2-\nu)\kappa^2/r_i^2\}/\lambda^3$

$$V_\theta=\left\{\begin{array}{ccccc} & & \bar{c}_1 & & \\ & \bar{c}_2 & \bar{c}_3 & \bar{c}_2 & \\ & & \bar{c}_4 & & \end{array}\right\} W \quad \cdots\cdots(10)$$

where

$\bar{c}_1=D\kappa\{(2\nu-1)\lambda/2r_i+2-\nu\}/2\lambda^3r_i$
$\bar{c}_2=D/2r_i^3\omega^3$
$\bar{c}_3=-D\kappa\{\kappa^2/r_i^2+(\nu-1)\lambda^2/r_i^2+2-\nu\}/\lambda^3r_i$
$\bar{c}_4=-D\kappa\{(2\nu-1)\lambda/2r_i+\nu-2\}/2\lambda^3r_i$

(2) Boundary Conditions

Boundary conditions of circular ring sector plates supported by edge-beams are presented here. The plate-beam system considered is shown in Fig. 2. The forces and moments acting at the

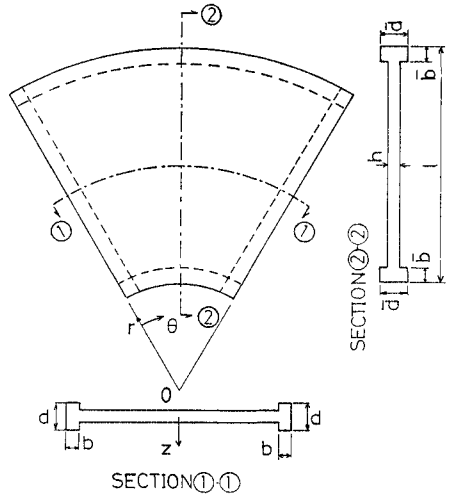

Fig. 2 Plate-Beam System

junctions of the plates and edge-beams are shown in Figs. 3 and 4. The plate is treated to be connected to the inner edge of the beam and is analysed by small deformation, thin plate theory. The edge-beams are analysed separately using simple bending and torsion theory, and it is assumed that the width of edge-beam $b(\bar{b})$ is sufficiently small as much as can be ignored.

a) Boundary Conditions along the Straight Edge-Beams

Referring to Fig. 3, two boundary equations

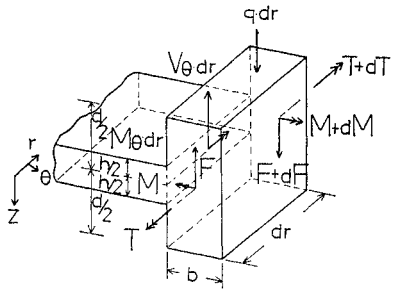

Fig. 3 Boundary Forces at Plate and Straight Beam Junction

are given along the edge $\theta=\theta_0$ as follows:

Equilibrium of forces in the z direction,

$$V_\theta - q - dF/dr = 0 \quad \cdots\cdots(11)$$

Equilibrium of moments about the r axis,

$$M_\theta + dT/dr = 0 \quad \cdots\cdots(12)$$

Eqs. (11) and (12) can be transformed into finite difference equations shown by Eqs. (13) and (14), respectively:

$$\left\{ \begin{array}{ccccccc} & & d_1 & & & & \\ & d_2 & & d_3 & & d_2 & \\ d_4 & & d_5 & & d_6 & & d_5 & & d_4 \\ & d_7 & & d_8 & & d_7 & \\ & & d_4 & & & & \end{array} \right\} W = \frac{q\lambda^3}{D} \quad \cdots\cdots(13)$$

where

$d_1 = H_r m$

$d_2 = \kappa\{1-\nu/2+(2\nu-1)\lambda/4r_i\}r_i$

$d_3 = -4d_1$

$d_4 = \kappa^3/2r_i^3$

$d_5 = -\kappa\{\kappa^2/r_i^2+2-\nu+(\nu-1)\lambda^2/r_i^2\}/r_i$

$d_6 = 6d_1$

$d_7 = \kappa\{1-\nu/2+(1-2\nu)\lambda/4r_i\}/r_i$

$$\left\{ \begin{array}{ccccc} & e_1 & & e_2 & & e_1 & \\ e_3 & & e_4 & & e_5 & & e_3 \\ & e_1 & & e_6 & & e_1 & \end{array} \right\} W = 0 \quad \cdots\cdots(14)$$

where

$e_1 = -J_r m$

$e_2 = -r_i(\lambda/r_i+2\nu)/\kappa$

$e_3 = 2(J_r m-\kappa/r_i)$

$e_4 = 4r_i(\kappa^2/r_i^2+\nu)/\kappa$

$e_5 = -2(J_r m+\kappa/r_i)$

$e_6 = r_i(\lambda/r_i-2\nu)/\kappa$

b) Boundary Conditions along the Curved Edge-Beams

Referring to Fig. 4, three boundary equations are given along the curved edge-beam as follows:

Equilibrium of forces in the z direction,

$$V_r + \bar{q} + d\bar{F}/ds = 0 \quad \cdots\cdots(15)$$

Equilibrium of moments about the θ axis,

$$d\bar{T}/ds + \bar{M}/R - M_r = 0 \quad \cdots\cdots(16)$$

Equilibrium of moments about the r axis,

$$d\bar{M}/ds - \bar{T}/R - \bar{F} = 0 \quad \cdots\cdots(17)$$

Elimination of $\bar{F}$ from Eqs. (15) and (17) will yield the following equation:

$$V_r + \bar{q} + d^2\bar{M}/ds^2 - 1/R \cdot d\bar{T}/ds = 0\,. \quad \cdots\cdots(18)$$

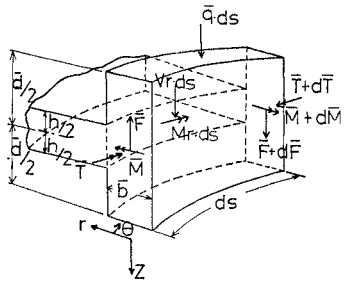

Fig. 4 Boundary Forces at Plate and Curved Beam Junction

Eqs. (16) and (18) can be transformed into finite difference equations shown by Eqs. (19) and (20), respectively:

$$\left\{ \begin{array}{ccccc} & f_1 & & f_2 & & f_1 & \\ f_3 & & f_4 & & f_5 & & f_3 \\ & f_1 & & f_5 & & f_1 & \end{array} \right\} W = 0 \quad \cdots\cdots(19)$$

where

$f_1 = -mJ_\theta/2\omega^2$

$f_2 = mH_\theta/2 + mJ_\theta/\omega^2 - R^2/\lambda^2 - \nu R/2\lambda$

$f_3 = m\lambda(H_\theta+J_\theta)/R\omega^2 - \nu/\omega^2$

$f_4 = -2m\lambda(H_\theta+J_\theta)/R\omega^2 + 2R^2/\lambda^2 + 2\nu/\omega^2$

$f_5 = -mH_\theta/2 - mJ_\theta/\omega^2 + \nu R/2\lambda - R^2/\lambda^2$

$$\left\{ \begin{array}{ccccccc} & & g_1 & & & & \\ & g_2 & & g_3 & & g_2 & \\ g_4 & & g_5 & & g_6 & & g_5 & & g_4 \\ & g_2 & & g_7 & & g_2 & \\ & & g_1 & & & & \end{array} \right\} W = \frac{\bar{q}\lambda^3}{D} \quad \cdots\cdots(20)$$

where

$g_1 = 1/2$

$$g_2=m\kappa^2(H_\theta+J_\theta)\lambda/2R^3+\kappa^2(2-\nu)/2R^2$$
$$g_3=-m(H_\theta+J_\theta)\kappa^2\lambda/R^3-1+\lambda/R-\lambda^2/2R^2-(2-\nu)\kappa^2/R^2$$
$$g_4=mH_\theta\kappa^4/R^4$$
$$g_5=\kappa^2(\nu-3)\lambda/R^3-m\kappa^2(4H_\theta\kappa^2+J_\theta\lambda^2)/R^4$$
$$g_6=2m\kappa^2(3H_\theta\kappa^2+J_\theta\lambda^2)/R^4-2\lambda\{R^2-(3-\nu)\kappa^2\}/R^3$$
$$g_7=m(H_\theta+J_\theta)\kappa^2\lambda/R^3+1+\lambda/R+\lambda^2/2R^2+(2-\nu)\kappa^2/R^2.$$

By assembling finite difference equations written for each interior mesh point in the network (using Eq. (6)) and the boundary equations written for edge points, simultaneous equations which contains the deflections of imaginary mesh points are obtained. The solution of these simultaneous equations gives the deflection at each mesh point. Using these deflections, the internal bending moments are evaluated by applying Eqs. (7) and (8).

(3) Rigidity Ratios

The span of plate measured in radial direction, the thickness of plate, the width of edge-beam and the depth of edge-beam are denoted by l, h, $b(\bar{b})$ and $d(\bar{d})$, respectively, as shown in Fig. 2. Using the five parameters α $(=l/h)$, β $(=d/b)$, $\bar{\beta}$ $(=\bar{d}/\bar{b})$, γ $(=b/h)$ and $\bar{\gamma}$ $(\bar{b}/h)$, the rigidity ratios H_r, H_θ, J_r and J_θ are expressed in Eqs. (21) to (24):

$$H_r=\frac{E_bI_b}{Dl}=(1-\nu^2)\frac{E_b\beta^3}{E_p\alpha}\gamma^4 \quad \cdots\cdots(21)$$

$$H_\theta=\frac{\bar{E}_b\bar{I}_b}{Dl}=(1-\nu^2)\frac{\bar{E}_b\bar{\beta}^3}{E_p\alpha}\bar{\gamma}^4 \quad \cdots\cdots(22)$$

$$J_r=\frac{G_bC_b}{Dl}=\frac{3(1-\nu)E_b}{8\alpha E_p}\gamma^4\beta\times\left[\frac{16}{3}-3.36\frac{1}{\beta}\left(1-\frac{1}{12\beta^4}\right)\right] \quad (\beta\geqq 1) \quad \cdots\cdots(23)$$

$$J_\theta=\frac{\bar{G}_b\bar{C}_b}{Dl}=\frac{3(1-\nu)\bar{E}_b}{8\alpha E_p}\bar{\gamma}^4\bar{\beta}\times\left[\frac{16}{3}-3.36\frac{1}{\bar{\beta}}\left(1-\frac{1}{12\bar{\beta}^4}\right)\right] \quad (\bar{\beta}\geqq 1) \quad \cdots\cdots(24)$$

where C_b and $\bar{C}_b$ are the approximate expressions proposed by R. J. Roark.[2)]

Results of numerical calculations for various values of these parameters will show the characteristics of the interactions between the sector plate and edge-beams.

(4) Method of Analysis of Plates Supported by Continuous Edge-Beams

Using the inverse of the coefficient matrix of unknown deflections, the plate supported by continuous edge-beams is easily analysed. The sector plate shown in Fig. 5 is analysed. The plate is supported by four continuous edge-beams along AB, BC, CD and DA, of which numbers of intermediate supports are denoted by s, v, t and y, respectively. Simultaneous equations for determining unknown intermediate reactions are expressed as follows:

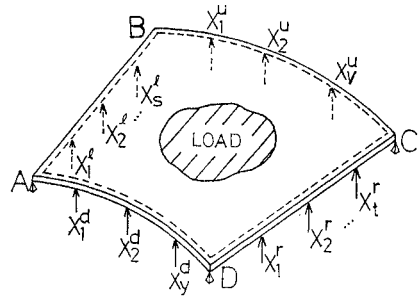

Fig. 5 Sector Plate Supported by Continuous Beams

$$\left.\begin{aligned}
&\sum_{i=1}^{s}X_i^l\delta_{ki}^l+\sum_{i=1}^{v}X_i^u\delta_{ki}^l+\sum_{i=1}^{t}X_i^r\delta_{ki}^l+\sum_{i=1}^{y}X_i^q\delta_{ki}^l\\
&=\delta_k^l-\eta_k^l \qquad (k=1,\cdots,s)\\
&\sum_{i=1}^{s}X_i^l\delta_{ki}^u+\sum_{i=1}^{v}X_i^u\delta_{ki}^u+\sum_{i=1}^{t}X_i^r\delta_{ki}^u+\sum_{i=1}^{y}X_i^q\delta_{ki}^u\\
&=\delta_k^u-\eta_k^u \qquad (k=1,\cdots,v)\\
&\sum_{i=1}^{s}X_i^l\delta_{ki}^r+\sum_{i=1}^{v}X_i^u\delta_{ki}^r+\sum_{i=1}^{t}X_i^r\delta_{ki}^r+\sum_{i=1}^{y}X_i^q\delta_{ki}^r\\
&=\delta_k^r-\eta_k^r \qquad (k=1,\cdots,t)\\
&\sum_{i=1}^{s}X_i^l\delta_{ki}^q+\sum_{i=1}^{v}X_i^u\delta_{ki}^q+\sum_{i=1}^{t}X_i^r\delta_{ki}^q+\sum_{i=1}^{y}X_i^q\delta_{ki}^q\\
&=\delta_k^q-\eta_k^q \qquad (k=1,\cdots,y)
\end{aligned}\right\} \quad \cdots\cdots(25)$$

where

X_i^l, X_i^u, X_i^r, X_i^q = support reaction at the intermediate point i on the continuous edge-beams AB, BC, CD and DA, respectively;

η_k^l, η_k^u, η_k^r, η_k^q = vertical displacement at the intermediate point k on the continuous edge-beams AB, BC, CD and DA, respectively;

δ_{ki}^l, δ_{ki}^u, δ_{ki}^r, δ_{ki}^q = deflection at the point k on the edge-beams AB, BC, CD and DA caused by the unit load acting on the point i, respectively;

δ_k^l, δ_k^u, δ_k^r, δ_k^q = deflection at the point k on the edge-beams AB, BC, CD and DA caused by the applied load, respectively.

Intermediate reactions X are determined by solving Eq. (25) simultaneously. Using these results, the deflections at each mesh point are evaluated in the similar way and internal forces of the plate are also determined by using these deflections.

3. NUMERICAL EXAMPLES

(1) Accuracy of Finite Difference Solution

Table 1 shows deflections and bending moments at the center of uniformly loaded sector plates. Two plates with different boundary conditions are studied here. One is simply supported along the four edges, and the other is simply supported along the two straight edges and free along the other two curved edges.

Table 1 clearly shows that the results obtained by finite difference techniques converge to exact solutions as the grid size is reduced. When the network in a plate contains 81 real mesh points, the solution is obtained with a sufficient degree of accuracy.

Table 1 Convergence of Results using Finite Difference Techniques ($\theta_0=\pi/6$, $\nu=0$, $\zeta=1$)

Boundary Conditions	Solution	w ($\times pl^4/D$)	M_r ($\times pl^2$)	M_θ ($\times pl^2$)
All edges simply supported	Finite difference techniques (81 points)	0.004037	0.03691	0.03575
	Finite difference techniques (121 points)	0.004037	0.03707	0.03587
	Fourier series	0.004037	0.03732	0.03598
Two straight edges simply supported and two curved edges free	Finite difference techniques (81 points)	0.01491	−0.006506	0.13252
	Finite difference techniques (121 points)	0.01484	−0.006537	0.13261
	Fourier series	0.01473	−0.006760	0.13306

In the following examples, except for Ex. 4, the network contains 9 by 9 points. In Ex. 4 the network contains 7 by 7 points.

(2) Single Span Sector Plates

Example 1 (Fig. 6)

The first numerical solution is presented for a uniformly loaded circular ring sector plate which is supported elastically by four edge-beams and simply supported at the four corner points.

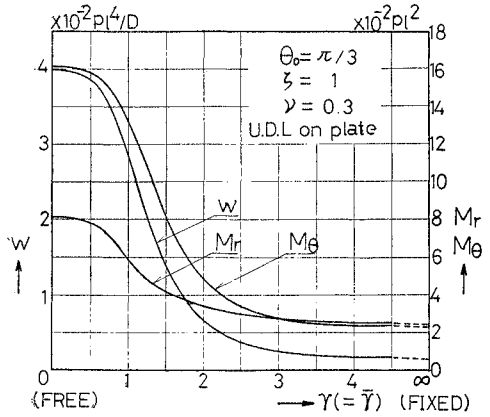

Fig. 6 Deflection and Bending Moments at the Center of the Plate (Ex. 1)

Parameters are adopted as follows:

$$\alpha=40,\quad \beta=\bar{\beta}=2 \quad \text{and} \quad \gamma=\bar{\gamma}=0\rightarrow\infty$$

where $\gamma=\bar{\gamma}=0$ means that all edges are free and $\gamma=\bar{\gamma}\rightarrow\infty$ means that all edges are fixed. Deflection w and bending moments M_r, M_θ at the center of the plate are shown in Fig. 6.

The values of w, M_θ and M_r of the plate with four fixed edges show decreases of 96.6%, 86.2% and 70.8%, respectively, compared with the corresponding values of the plate with four free edges.

Example 2 (Fig. 7)

The boundary and loading conditions of a plate are the same as those of Ex. 1, but its corner points are clamped in this example. Deflections and bending moments at the center of the plate

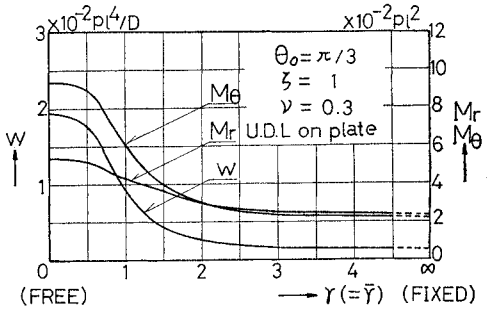

Fig. 7 Deflection and Bending Moments at the Center of the Plate (Ex. 2)

Table 2 Deflections and Bending Moments at the Center of the Plate
($H_r=H_\theta=H$, $J_r=J_\theta=J$)

	Ex.	$\gamma=\bar{\gamma}=0$ ($H=J=0$)		$\gamma=\bar{\gamma}=1$ ($H=0.1820$, $J=0.0481$)		$\gamma=\bar{\gamma}=1.5$ ($H=0.9214$, $J=0.2433$)		$\gamma=\bar{\gamma}=2$ ($H=2.912$, $J=0.769$)		$\gamma=\bar{\gamma}=3$ ($H=14.74$, $J=3.893$)		$\gamma=\bar{\gamma}=\infty$ ($H=J=\infty$)	
w	1	3.975	1	2.826	1	1.389	1	0.6508	1	0.2488	1	0.1356	1
	2	1.932	0.486	0.938	0.332	0.4479	0.322	0.2704	0.415	0.1686	0.678	0.1356	1.000
M_r	1	8.033	1	5.823	1	4.099	1	3.408	1	2.690	1	2.346	1
	2	5.362	0.667	4.337	0.745	3.637	0.887	3.061	0.898	2.545	0.946	2.346	1.000
M_θ	1	16.05	1	13.16	1	8.180	1	4.786	1	2.769	1	2.211	1
	2	9.362	0.583	6.106	0.464	4.011	0.490	3.067	0.641	2.437	0.880	2.211	1.000

w: $\times 10^{-2}\, pl^4/D$ $\quad M_r, M_\theta$: $\times 10^{-2}\, pl^2$

are shown in Fig. 7. Comparing the results for $\gamma=\bar{\gamma}\to\infty$ with those for $\gamma=\bar{\gamma}=0$, w, M_θ and M_r show decreases of 93.0%, 76.4% and 56.2%, respectively.

Their values decrease rapidly between $\gamma(\bar{\gamma})=0.5$ and $\gamma(\bar{\gamma})=3.0$ in both examples. Deflections and bending moments for $\gamma(\bar{\gamma})\geqq 4$ are nearly equal to those for $\gamma(\bar{\gamma})\to\infty$.

Ratios of values in Ex. 2 to those in Ex. 1 are given in Table 2. This table shows that supporting conditions of the corner points give remarkable effects on w, M_r and M_θ. Particularly the effect is most remarkable in w, and least in M_r. Ratios take the minimum values in case of $\gamma(\bar{\gamma})=1.5$ for w, $\gamma(\bar{\gamma})=1$ for M_θ and $\gamma(\bar{\gamma})=0$ for M_r.

Example 3 (Fig. 8)

In this example the following uniformly loaded sector plate is studied:

straight edges: simply supported,
curved edges : supported elastically by edge-beams,

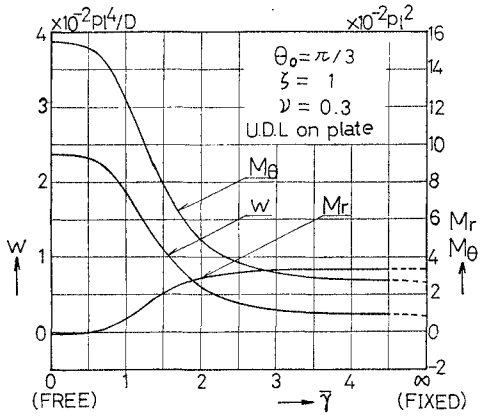

Fig. 8 Deflection and Bending Moments at the Center of the Plate (Ex. 3)

corner points : curved edge-beams are fixed for torsion and simply supported for bending.

Parameters $\alpha=40$, $\bar{\beta}=2$, $\bar{\gamma}=0\to\infty$ are used. The condition of two straight edges are expressed by $H_r\to\infty$ and $J_r=0$.

Deflection and bending moments at the center of the plate decrease rapidly in the region of $0.5\leqq\bar{\gamma}\leqq 3.0$, but these values do not vary for $\bar{\gamma}\geqq 4.0$ as shown in Fig. 8.

Example 4 (Figs. 9 to 15)

The following two uniformly loaded sector plates shown in Fig. 9 are studied in this example:

(Case A)
straight edges: supported elastically by simple beams,
curved edges : free.

(Case B)
straight edges: supported elastically by two-span continuous beams,
curved edges : free.

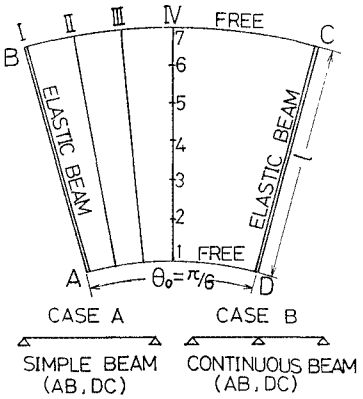

Fig. 9 Plate Geometry

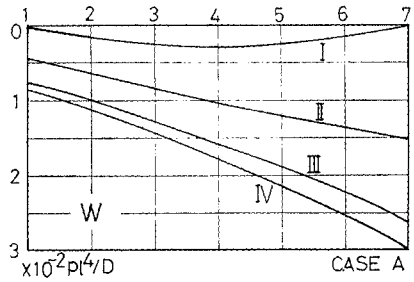

Fig. 10 Deflection of the Plate Supported by Simple Beams

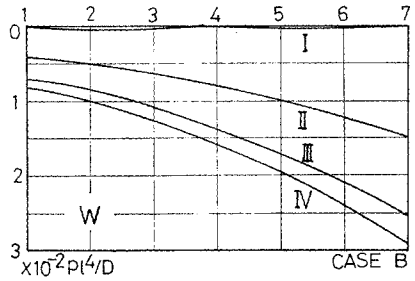

Fig. 11 Deflection of the Plate Supported by Continuous Beams

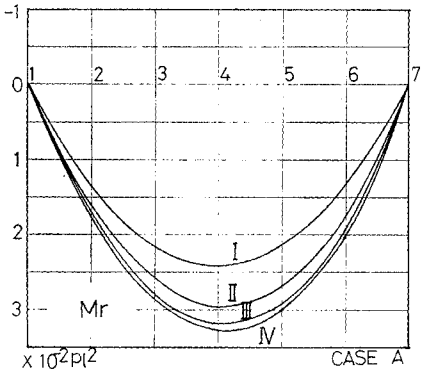

Fig. 12 Bending Moment in Radial Direction of the Plate Supported by Simple Beams

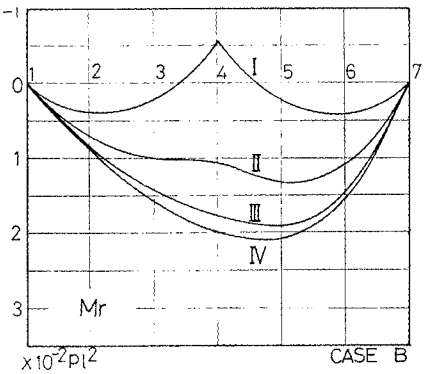

Fig. 13 Bending Moment in Radial Direction of the Plate Supported by Continuous Beams

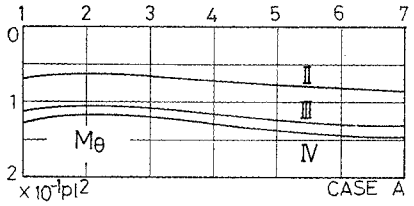

Fig. 14 Bending Moment in Tangential Direction of the Plate Supported by Simple Beams

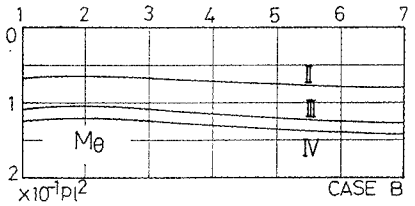

Fig. 15 Bending Moment in Tangential Direction of the Plate Supported by Continuous Beams

Rigidity ratios $H_r=1.67$, $J_r=0$ and $H_\theta=J_\theta=0$ are adopted.

Deflections and bending moments along the line I, II, III and IV are shown in Figs. 10 to 15. When deflections and bending moments at the center of the plate in Case B are compared with those in Case A, w and M_r show decreases of 11.2% and 39.8%, respectively. The values of M_θ in both cases are almost equal.

The intermediate support reaction in Case B is 26.5% of total applied load.

(3) Two-Span Continuous Sector Plates

Example 5 (Figs. 16 and 17)

The circular ring sector plate shown in Fig. 16 is a two-span continuous plate in tangential direction, and carries a uniformly distributed load p. Curved edges are supported elastically by edge-beams and straight edges are supported on knife-edges.

Parameters $\alpha=40$, $\bar{\beta}=2$ and $\bar{\gamma}=0\rightarrow\infty$ are introduced.

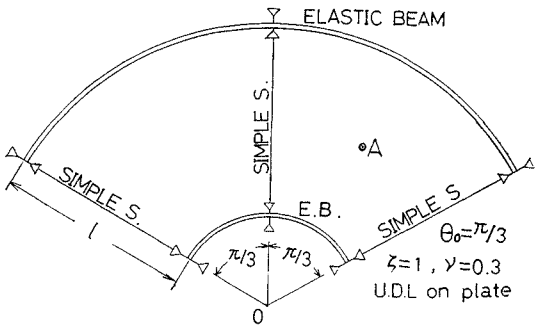

Fig. 16 Continuous Plate Geometry

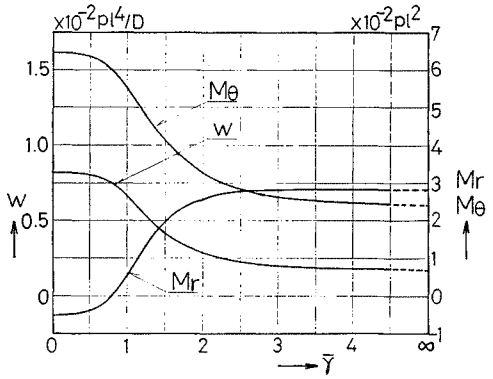

Fig. 17 Deflection and Bending Moments at the Central Point A of the Continuous Plate

Deflection and bending moments at the central point A of the plate are shown in Fig. 17. The feature of three curves is similar to those of Ex. 3.

Example 6 (Fig. 18)

The boundary and loading conditions of the plate are the same as those of Ex. 5 except for the values of $\bar{r}$, ζ and θ_0. In this example $\bar{r}=$ 1.5 and $\zeta=2$. The opening angle θ_0 is varied from 0° to 90°.

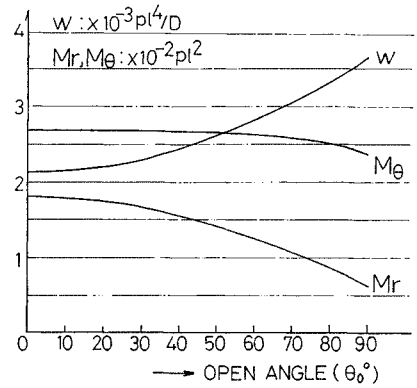

Fig. 18 Effect of the Open Angle on the Deflection and Bending Moments

Fig. 18 shows deflection and bending moments at the central point A which do not vary in the region of $0°\leqq\theta_0\leqq20°$. For the values of θ_0 larger than 20°, w steeply increases, M_r steeply decreases and M_θ gradually decreases and M_θ gradually decreases. When these values for $\theta_0=90°$ are compared with those for $\theta_0=0°$, w shows an increase of 71.1%, M_r and M_θ show decreases of 65.2% and 10.9%, respectlveiy.

4. CONCLUSIONS

Finite difference analysis of circular ring sector plates supported by edge-beams are presented in this paper.

As rigidity ratios are introduced into boundary conditions derived at the junctions of the plates and edge-beams, the sector plates with various boundary conditions can be easily analysed by varying these rigidity ratios. When a sector plate is supported by continuous edge-beams, the plate can be easily analysed by using the inverse of the coefficient matrix of unknown deflections for the plate with simply supported edge-beams. Furthermore, this analysis is applicable to continuous sector plates with edge-beams.

Computational results obtained for various values of these ratios show the characteristics of the interactions between the sector plates and the supporting conditions of their edges.

From numerical calculations for many typical cases, the following conclusions may be drawn.

1) When a plate carries a uniformly distributed load, the network of 9 by 9 points gives a sufficient accuracy as shown in Table 1.

2) Supporting conditions at the corner points of the plates and flexural and torsional rigidities of the edge-beams give remarkable effects on w, M_r and M_θ of the plates as shown in Table 2.

3) In the region of small rigidity ratios, deflections and bending moments vary remarkably. But when the rigidity ratios become larger than certain values, w, M_r and M_θ do not vary any more as shown in Figs. 6, 7, 8 and 17.

4) In the case of the plate is simply supported along the straight edges and free along the curved edges, the value of M_r at the center of the plate has a negative value as shown in Fig. 8.

5) The variation of opening angle give also remarkable effects on w, M_r and M_θ as shown in Fig. 18. Particularly the effect is remarkable in w and M_r.

The results obtained here for various support-

ing conditions at the corner points of the plates, flexural and torsional rigidities of the edge-beams and opening angles of the plates seem to be useful in design of sector plates sopported by edge-beams.

ACKNOWLEDGEMENT

The author wishes to express his thanks to Dr. T. Yoshimura, Prof. of Kyushu Univ., Dr. T. Chisyaki, Assoc. Prof. of Kyushu Univ., Mr. H. Hikosaka, Lect. of Kyushu Univ. and Dr. T. Kaneko, Research Engr. in Kawasaki Steel Co., for their valuable suggestions.

REFERENCES

1) Yoshimura, J.: The bending of curvilinear orthotropic circular ring sector plate, Trans. of JSCE, No. 82, June, 1962.
2) Roark, R. J.: Formulas for Stress and Strain, pp. 174, McGraw-Hill Book Co., 1954.
3) Khan, M. A. and K. O. Kemp: Elastic full composite action in a slab and beam system, The Structural Engineer, Vol. 48, No. 9, Sept., 1970.
4) Kaneko, T. and H. Otsuka: Analysis of circular ring sector plates with two opposite straight edges elastically supported by frames, Technology Reports of the Kyushu University, Vol. 45, No. 1, Jan., 1972.
5) Otsuka, H. and T. Kaneko: Analysis of circular ring sector plates with all edges elastically supported by frames, Technology Reports of the Kyushu University, Vol. 45, No. 6, Dec., 1972.

NOTATIONS

The following symbols are used in this paper:

$b, \bar{b}$ =width of straight and curved edge-beams, respectively;
$D=E_p h^3/12(1-\nu^2)$=flexural rigidity of plate per unit width;
$d, \bar{d}$ =depth of straight and curved edge-beams, respectively;
E_p =Young's modulus of plate material;
$E_bI_b, \bar{E}_b\bar{I}_b$=flexural rigidity of straight and curved edge-beams, respectively;
$F, \bar{F}$ =vertical shear force on straight and curved edge-beams, respectively;
$G_bC_b, \bar{G}_b\bar{C}_b$=torsional rigidity of straight and curved edge-beams, respectively;
h =thickness of plate;
$H_r=E_bI_b/Dl$=ratio of flexural rigidity of straight edge-beam to plate width;
$H_\theta=\bar{E}_b\bar{I}_b/Dl$=ratio of flexural rigidity of curved edge-beam to plate width;
(i, j) =a number of mesh point under consideration;
$J_r=G_bC_b/Dl$=ratio of torsional rigidity of straight edge-beam to flexural rigidity of plate width;
$J_\theta=\bar{G}_b\bar{C}_b/Dl$=ratio of torsional rigidity of curved edge-beam to flexural rigidity of plate width;
$l=R_0-R_i$=span of plate in radial direction;
$M, \bar{M}$ =bending moment on the straight and curved edge-beams in the vertical planes, respectively;
M_r, M_θ =bending moment per unit width of the plate in the radial and tangential directions, respectively;
m, n =number of division in the radial and tangential directions, respectively;
p =intensity of the applied load on the plate;
$q, \bar{q}$ =vertical load on the straight and curved edge-beams per unit length, respectively;
(r, θ, z) =cylindrical coordinates;
R =radius of curved edge-beam;
R_i, R_0 =radius of internal and external plate edges, respectively;
r_i =distance between a central point 0 of cylindrical coordinates and mesh point (i, j);
$T, \bar{T}$ =twisting moment on the straight and curved edge-beams, respectively;
V_r, V_θ =reaction force per unit width of the plate in the radial and tangential directions, respectively;
w =deflection along the z-direction;
$\alpha=l/h$ =ratio of span of plate in radial direction to thickness of plate;
$\beta=d/b$, $\bar{\beta}=\bar{d}/\bar{b}$=depth to width ratio of straight and curved edge-bems, respectively;
$\gamma=b/h$ =ratio of width of straight edge-beam to thickness of plate;
$\bar{\gamma}=\bar{b}/h$ =ratio of width of curved edge-beam to thickness of plate;
Δ =Laplacian operator in polar coordinate system;
$\zeta=(R_0+R_i)\theta_0/2l$=ratio of central circular arc length to span of the plate in radial direction;
θ_0 =opening angle of plate;
λ =radial spacing of mesh pattern in radial direction;
ν =Poisson's ratio for plate material;
ω =Polar arc of mesh pattern in tangential direction.

(*Received Jan. 30, 1973*)